Non-Linear Finite Element Modeling of THUNDER Piezoelectric Actuators

Barmac K. Taleghani[1], Joel F. Campbell[2]

[1]Army Research Laboratory, Vehicle Technology Center, MS 230
NASA Langley Research Center, Hampton, VA 23681-0001

[2]Science Applications International Corporation
1 Enterprise Parkway Suite 300
Hampton, VA 23681-0001

ABSTRACT

A NASTRAN non-linear finite element model has been developed for predicting the dome heights of THUNDER (**TH**in Layer **UN**imorph Ferroelectric **D**riv**ER**) piezoelectric actuators. To analytically validate the finite element model, a comparison was made with a non-linear plate solution using Von Karmen's approximation. A 500 volt input was used to examine the actuator deformation. The NASTRAN finite element model was also compared with experimental results. Four groups of specimens were fabricated and tested. Four different input voltages, which included 120, 160, 200, and 240 Vp-p with a 0 volts offset, were used for this comparison.

Keywords: NASTRAN, finite element, non-linear, THUNDER, piezoelectric, actuator

1. INTRODUCTION

THUNDER [1] is a piezoelectric actuator that was developed at the NASA Langley Research Center. THUNDER (Fig. 1) provides significantly larger displacements than available previously, and the actuator exhibits a displacement-to-weight ratio orders of magnitude greater than any other actuator today. The efficiency of this design has made this type of actuator attractive for applications such as air pumps, speakers, motors and many others.

In order to use such devices in engineering applications, modeling and characterization are essential. There have been no simple analytical models available to understand THUNDER's static and dynamic behavior. The major features which determine the operating parameters of a THUNDER actuator are the type and thickness of piezo-ceramic, the curvature, number of layers, thickness and placement of the foil stressing member, the adhesive, and thickness. The objective of this research is to develop a non-linear NASTRAN [2] finite element model to capture the influence of the above-cited features and to analytically predict doming of the actuator during the manufacturing process and due to applied voltages. A simple approach is used in which temperature-induced expansion is used to simulate voltage actuation as described by Freed and Babuska [3].

---

[1] B. K. Taleghani: Email: b.k.taleghani@larc.nasa.gov
[2] J. F. Campbell: E-mail: joel.f.campbell@larc.nasa.gov

2. DESCRIPTION OF THUNDER PROCESS

To fabricate the THUNDER specimens (Fig. 2) used in this study, a 6.8 mil PZT-5A ceramic is bonded to a sheet of stainless steel and a sheet of 1 mil aluminum using a 1mil sheet of LaRC-SI at the top and bottom of the PZT ceramic. The consolidating of the layers is done in an autoclave at a temperature of 325 degrees C with a pressure of 100 psi. As the autoclave cools, the LaRC-SI consolidates but since there is a mismatch in the coefficient of thermal expansion (CTE) between the aluminum, PZT ceramic, and stainless steel, the consolidated assembly takes a curved shape due to different thermal strains in the ceramic and metals.

3. MODELING APPROACH

A NASTRAN non-linear finite element model was developed for predicting dome heights resulting from fabrication and applied voltages to the PZT layer. The finite element model assumed that at the transition temperature of LaRC-SI (assumed to be 250 degrees C), all layers are bonded. The bonding constrains all layers to move together while the specimen is cooled, thus generating thermal stresses due to differing CTE's in the layers. This bonding was modeled by attaching the layers together using rigid bars. The model only accounts for the process where the device was cooled from 250 degrees C to room temperature (25 degrees C).

The model is divided into two parts. The first part is the modeling of the fabrication cooling process where the initial doming occurs. The thermal strain resulting from cooling was calculated as follows

$$\varepsilon_{thermal} = \alpha \Delta T \tag{1}$$

where $\varepsilon_{thermal}$ is the thermal strain due to the cooling process, α is the coefficient of thermal expansion, and ΔT is the temperature difference.

The second part models the strain resulting from the applied voltage, which was determined as follows

$$\varepsilon_{piezo} = d_{31} \frac{V}{t_{pzt}} \tag{2}$$

where ε_{piezo} is the piezoelectric strain, d_{31} is the piezoelectric charge constant, V is the applied voltage, and t_{PZT} is the thickness of the PZT layer.

In order to incorporate the voltage effects into the NASTRAN a simple thermal analogy was used. The piezoelectric charge constant d_{31} divided by PZT ceramic thickness was an equivalent coefficient of thermal expansion, and voltage is equivalent to a temperature difference. That is,

The total strain is given by

$$\varepsilon_{total} = \varepsilon_{piezo} + \varepsilon_{thermal} \tag{3}$$

4. SPECIMENS FOR COMPARISON OF NASTRAN MODEL WITH NON-LINEAR PLATE SOLUTION

To validate the non-linear NASTRAN finite element model, comparison was made between the NASTRAN model and the non-linear plate solution [4], which used Von Karmen approximation. Two specimens were used for this comparison. The lay-up configurations for these two specimens are shown in Fig. 2. The first specimen was 3.0 inches long and 1.5 inches wide, and the second was 2.5 inches long and 1 inch wide. Both specimens included the same lay-up shown in figure 2. The material properties and the lay-ups for the above comparison are shown in Table 1.

5. TEST SPECIMENS FOR COMPARISON OF NASTRAN MODEL WITH EXPERIMENTAL RESULTS

To compare the non-linear NASTRAN finite element model with experimental results, four groups of specimens were fabricated and tested. The material properties and the lay-ups for the above comparison are shown in Table 2 (a) and (b). The length and width of the first and second group were 1 inch by 1 inch, respectively. The lay-up configurations in all the groups were the same, with the exception of their respective base metal thicknesses, which was 3 mils for the first group and 5 mils for the second group. The length and width of the third and fourth groups were 2 inches by 1 inch, respectively. These two groups had similar lay-up configuration and base metal thicknesses as the first and second groups.

6. FINITE ELEMENT MODEL DESCRIPTION

The model geometry was developed and meshed using I-DEAS [5] Master Series Version 6.0. Creating all the layers and stacking them developed the 3D-geometry model. A mid-surface was then created on each layer for elements to be placed. After meshing was completed, the midsurfaces were connected using rigid bars as shown in Fig. 3.

The NASTRAN model, which was used to compare with the non-linear plate model, consisted of 250 CQUAD4 plate elements, 330 nodes, 264 rigid elements RBAR's, and 1800 degrees of freedom. For the comparison between the NASTRAN model and measured results, the models for the first and second groups consisted of 320 CQUAD4 quadrilateral plate elements, 324 rigid elements, 405 nodes, and 2000 degrees of freedom. The models for the third and fourth groups included 240 CQUAD4 plate elements, 252 rigid elements, 315 nodes, and 1800 degrees of freedom. SOL 106 was used for non-linear static thermal analysis. In order to assure convergence, the temperature range was divided into ten segments. The assumption was made that at 250 degrees C the layers are bonded and consolidated. Therefore, the cooling process was modeled from 250 degrees C to 25 degrees C.   RBAR's were used to model this bonding. Since RBAR's were connected together, there exist independent and dependent degrees of freedom on nodes connected by RBAR's. The nodes on the stainless steel mid-layer had the independent degrees of freedom, and all the nodes on other layers had the dependent degrees of freedom. Free-free boundary conditions were used for the analysis. TEMP (INIT) and TEMP (LOAD) were used to assign initial and final temperature loads to TEMPD cards.   The model included two subcases. The initial part modeled the fabrication cooling process. The second part includes keeping all grid points at room temperature, while voltages (as equivalent temperatures) were added to elements on the PZT layers by using TEMPP1 cards. Upon completion of the NASTRAN analysis, the results were migrated to I-DEAS for graphical presentation.

7. RESULTS

7.1 NASTRAN vs. Non-linear Plate Solution

Dome heights due to the curing process and voltage inputs were compared for both specimens in the longitudinal and transverse directions. The dome heights in the transverse and longitudinal directions were used for this comparison. In order to calculate the dome heights at the cure state and due to input voltage in the transverse direction the model was constrained on one edge parallel to the length and allowed to move at the other edge and dome. The comparisons are shown in Tables 3(a) and (b). For the devices shown in Table 3 (a), the best comparison of the dome heights at the cure state belonged to the 2 mil stainless steel base, which had a difference of 5.5%. The largest difference was in the comparison of dome heights due to voltage input for the 3 mil base stainless steel base, which was 7.3%.

For the transverse direction, the best comparison occurred during the input voltage for the 3 mil stainless steel base, which was 3.6%. The largest difference in this group was for the 2 mil base at the cured state, which was 12.0%. The dome heights in the longitudinal as well as transverse direction for this group compared very well. For specimens 2.5 inches by 1.0 inches shown in Table 3 (b), comparison of dome heights in longitudinal direction, the largest difference belonged to 2 mil base at cured state which was 13.4%, and the closest comparison belonged to 2 mil base during the input voltage which was 8.5%.
In the transverse direction the best correlation among this group belonged to the specimen with the 2 mil base during the induced voltage which was 3.6%, and the largest was 15.8% for the specimen with 3 mil base at cure state.

7.2 NASTRAN Predictions vs. Experimental Data.

Experimental measurements on NASA-fabricated THUNDER wafers were made by NASA Langley researchers from the Composite and Polymers Branch and the Data Systems and Instrument Support Branch. Their preliminary data is used in this paper as a comparison with the numerical results. Refinements to the experimental set-up and test fixtures are underway, and improved results will be published elsewhere at a later date.

A number of THUNDER wafers of various sizes were driven at 1 Hz at voltages of 120,160,200, and 240 volts peak-to-peak (Vp-p) with a 0 volts offset. The wafers were mounted using an adhesive tape in a manner to constrain lateral movement but allow vertical displacement. This mounting technique can introduce non-repeatable effects in the displacement data which future improvements should alleviate. A fiber optic sensor was placed above the wafer to measure the vertical displacement. The range of the sensor was 50 mils with micro-inch resolution at 1 Hz.

The results are shown in Tables 4 and Fig. 4. As shown in Table 4(a), the largest difference among dome heights occurred at the cure state which was 25.9%. However, comparisons due to the input voltage for this group showed very good correlation for the 120 Vp-p and for 160 Vp-p. The largest difference was due to 240 Vp-p, which was 7.9%. For the second group in Table 4(b), the dome height differences at the cure state was 23.5%. The comparison of dome heights due to input voltages for this group was almost the same with the exception of 240 Vp-p, which was 5.5%. This group exhibited the best correlation among the four groups.
The third group in Table 4(c) had very good agreement in dome heights at the cured state, which was 4.6%. The dome heights during input voltage for this group ranged from 1.4% to 17.6%.
The fourth group in Table 4(d) had the best correlation at the cure state. However, the dome height comparison due to input voltages ranged from 8.3% to 21.6%.

The first and second group showed a good correlation of measured and calculated data for induced voltages. However, the comparison of dome heights at curing was 25.9% and 23.5%, respectively. This was probably due to variations in specimens due to the manufacturing process where the LaRC-SI had a

wider thickness in top layer. The above specimens were cut and photographed. The variations in LaRC-SI thicknesses may be seen in Fig. 5. Figure 5 shows two random samples of test specimens, denoted I and II. Note the large differences in the LaRC-SI layers.

8. SUMMARY

A NASTRAN non-linear finite element model was developed for predicting dome heights of THUNDER piezoelectric actuators due to fabrication and voltage input. The model was compared with the non-linear plate solution using the Von Karmen approximation. The NASTRAN finite element model was also compared with experimental results. The differences between analyses ranged between 3% and 16%. The differences between analysis and test at the cured state ranged between 0 and 26%. The differences between analysis and test for voltage input ranged between 0 to 22%. The largest differences between analysis and test for doming in the cured state was thought to be due to variations in the manufacturing process for the test articles.

ACKNOWLEDGEMENTS

REFERENCES

1. R. G. Bryant, K. M. Mossi, G. V. Selby, "Thin-layer Composite Unimorph ferroelectric driver and sensor properties." Materials Letters, August 1997.

2. L. H. Sang, MSC / NASTRAN Handbook for Non-Linear analysis, The MacNeil Schwendler Corporation, 1992.

3. V. Babuska and B. D. Freed "Finite Element Modeling of Composite Piezoelectric Structures with MSC/NASTRAN." Proceedings, SPIE Smart Structures and Materials. Paper 3041-60 March 1997.

4. J. F. Campbell, "Quasi-Static Analysis of THUNDER Actuator", to be published in Smart Structures and Materials Journal.

5. I-DEAS Simulation User's Guide, Structural Dynamics Research Corporation, 1996.

Sample size (3.0" x1.5") and (2.5" X1.0")

	Material	Thickness (in.)	Modulus of Elasticity (E) (psi) $\times 10^6$	Coefficient of Thermal Expansion(CTE) $10^{-6}/^0C$
Layer 1 (Top Layer)	Aluminum	0.001	10	24.0
Layer 2	LaRC-SI	0.001	0.58	46
Layer 3	PZT 5A	0.0068	9	1.5
Layer 4	LaRC-SI	0.001	0.58	46
Layer 5 (Bottom layer)	Stainless Steel	0.002 and 0.003	38	17.3

Table 1. Lay-ups and Material Properties for comparison of NASTRAN Non-linear model versus Non-linear plate solution

(a) Specimen size 1"x1"

	Material	Thickness (in.)	Modulus of Elasticity (E) (psi) $\times 10^6$	Coefficient of Thermal Expansion(CTE) $10^{-6}/^0C$
Layer 1 (Top Layer)	Aluminum	0.001	10	24.0
Layer 2	LaRC-SI	0.001	0.58	46
Layer 3	PZT 5A	0.0068	9	1.5
Layer 4	LaRC-SI	0.001	0.58	46
Layer 5 (Bottom layer)	Stainless Steel	0.003 and 0.005	38	17.3

(b) Specimen size 2"x1"

	Material	Thickness (in.)	Modulus of Elasticity (E) (psi) $\times 10^6$	Coefficient of Thermal Expansion(CTE) $10^{-6}/^0C$
Layer 1 (Top Layer)	Aluminum	0.001	10	24.0
Layer 2	LaRC-SI	0.001	0.58	46
Layer 3	PZT 5A	0.0068	9	1.5
Layer 4	LaRC-SI	0.001	0.58	46
Layer 5 (Bottom layer)	Stainless Steel	0.003 and 0 0.005	38	17.3

Table 2. Lay-ups and Material Properties for comparison between NASTRAN Non-linear model and experimental results

(a) THUNDER device size: 3.0 x 1.5

Dome heights in Longitudinal direction	Base metal Thickness	Plate Solution (in)	NASTRAN (in)	% difference
At Curing	2 mil	0.292	0.275	5.8
	3 mil	0.334	0.310	7.2
Induced Voltage (500 V)	2 mil	0.237	0.224	5.5
	3 mil	0.275	0.255	7.3

Dome heights in Transverse direction	Base metal Thickness	Plate Solution (in)	NASTRAN (in)	% difference
At Curing	2 mil	0.074	0.083	12.0
	3 mil	0.085	0.094	10.6
Induced Voltage (500 V)	2 mil	0.061	0.068	11.5
	3 mil	0.028	0.029	3.6

(b) THUNDER device size: 2.5 x 1.0 inches

Dome heights in Longitudinal direction	Base metal Thickness	Plate Solution (in)	NASTRAN (in)	% difference
At Curing	2 mil	0.202	0.175	13.4
	3 mil	0.231	0.202	12.6
Induced Voltage (500 V)	2 mil	0.164	0.150	8.5
	3 mil	0.200	0.178	11.0

Dome heights in Transverse direction	Base metal Thickness	Plate Solution (in)	NASTRAN (in)	% difference
At Curing	2 mil	0.034	0.036	5.9
	3 mil	0.038	0.044	15.8
Induced Voltage (500 V)	2 mil	0.028	0.029	3.6
	3 mil	0.032	0.035	9.4

Table 3. Comparison of NASTRAN Finite Element Results to the Non-linear Plate Solution

(a) First group (1"x 1", 3mil Stainless Steel)

Curing Dome Height:

Measured Dome Height (in.)	Calculated Dome Height (in.)	% Difference
0.054	0.040	25.9

Induced Voltages Dome Height:

Voltage Vp-p	Measured Peak to Peak Displacements (in.)	Calculated Peak to Peak Displacements (in.)	% Difference
120	0.0017	0.0017	-
160	0.0024	0.0024	-
200	0.0030	0.0029	3.2
240	0.0038	0.0035	7.9

(b) Second Group (1"x 1", 5mil Stainless Steel)

Curing Dome Height:

Measured Dome Height (in.)	Calculated Dome Height (in.)	% Difference
0.051	0.039	23.5

Induced Voltages Dome Height:

Voltage Vp-p	Measured Peak to Peak Displacements (in.)	Calculated Peak to Peak Displacements (in.)	% Difference
120	0.0016	0.0016	-
160	0.0023	0.0023	-
200	0.0028	0.0028	-
240	0.0036	0.0034	5.5

(c) Third Group (2"x 1", 3mil Stainless Steel)

Curing Dome Height:

Measured Dome Height (in.)	Calculated Dome Height (in.)	% Difference
0.152	0.145	4.6

Voltages Dome Height:

Voltage Vp-p	Measured Peak to Peak Displacements (in.)	Calculated Peak to Peak Displacements (in.)	% Difference
120	0.0069	0.0070	1.4
160	0.0091	0.0090	1.0
200	0.013	0.012	7.7
240	0.017	0.014	17.6

(d) Fourth Group (2"x 1", 5mil Stainless Steel)

Curing Dome Height:

Measured Dome Height (in.)	Calculated Dome Height (in.)	% Difference
0.143	0.143	-

Induced Voltages Dome Height:

Voltage Vp-p	Measured Peak to Peak Displacements (in.)	Calculated Peak to Peak Displacements (in.)	% Difference
120	0.0052	0.006	15.3
160	0.0074	0.009	21.6
200	0.0095	0.011	15.7
240	0.012	0.013	8.3

Table 4. Comparison of NASTRAN Finite Element predictions with Experimental Data
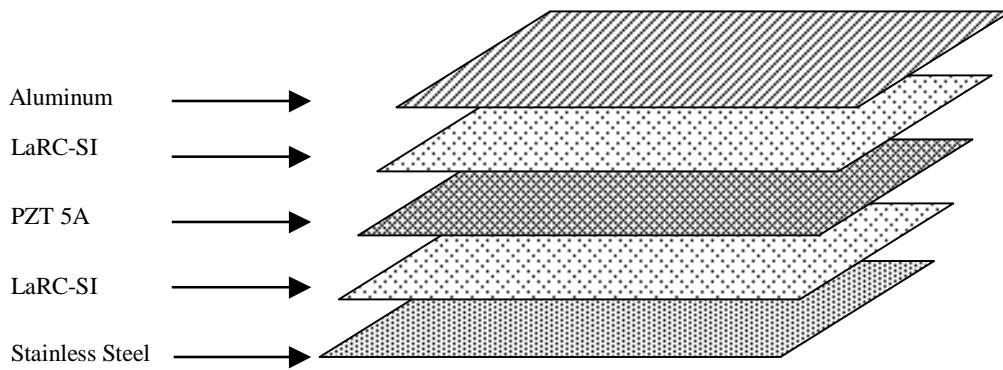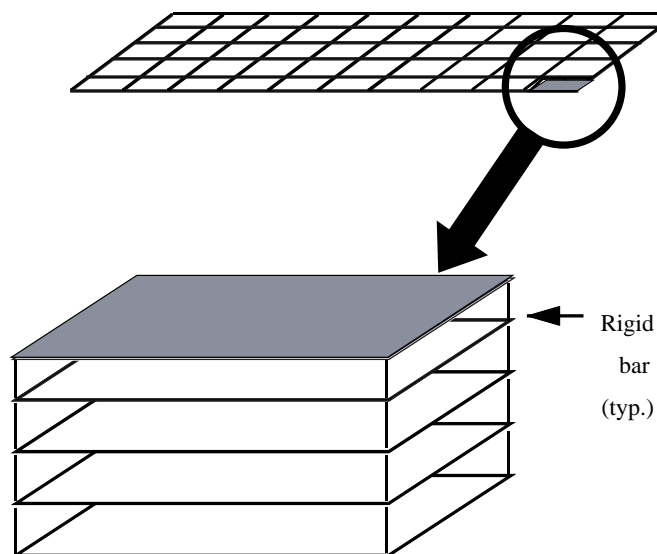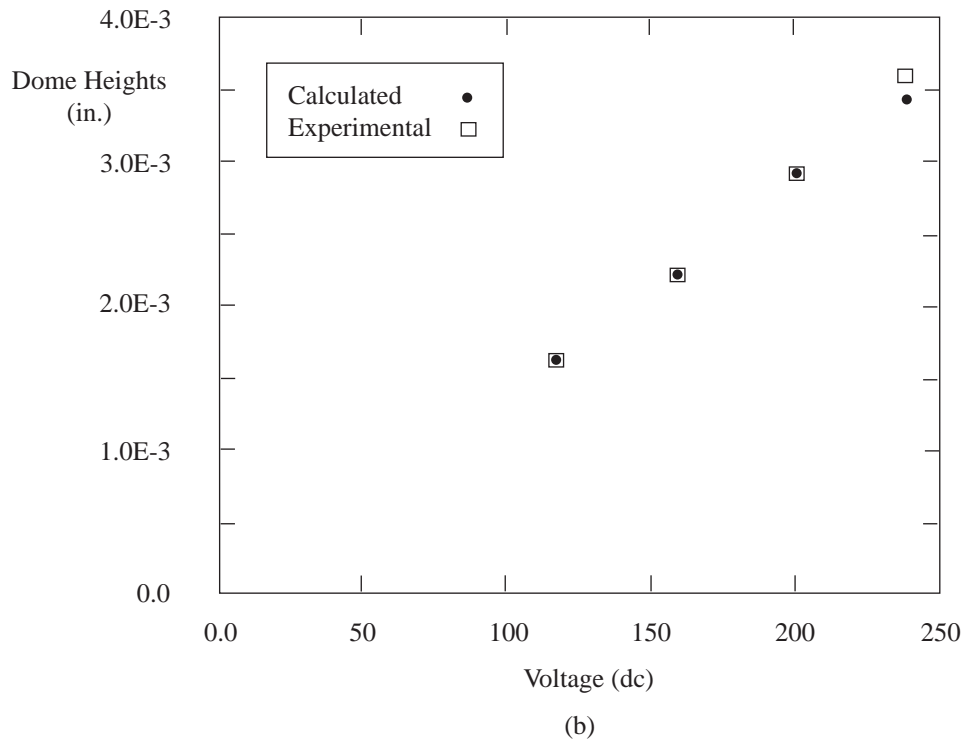
Fig. 1 THUNDER Device Longitudinal direction
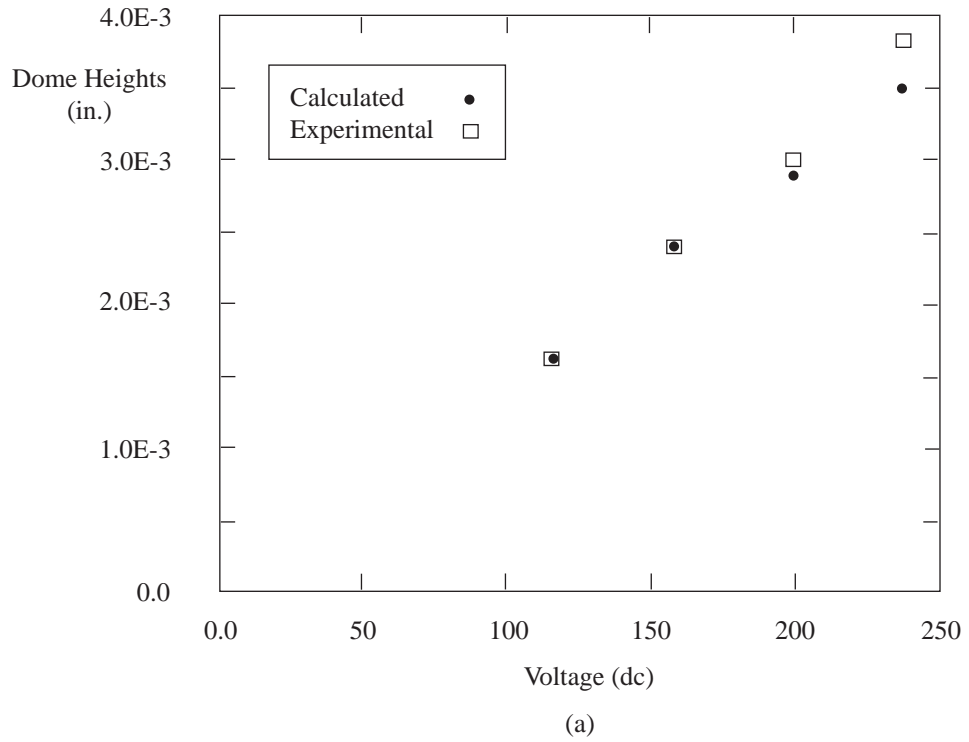
Aluminum

LaRC-SI

PZT 5A

LaRC-SI

Stainless Steel

Fig. 2 THUNDER Lay-up

Rigid bar (typ.)

Fig. 3 Rigid bars

(a)

4.0E-3

Dome Heights
(in.)

| Calculated | ● |
| Experimental | □ |

3.0E-3

2.0E-3

1.0E-3

0.0

0.0   50   100   150   200   250

Voltage (dc)

(a)

(b)

4.0E-3

Dome Heights
(in.)

| Calculated | ● |
| Experimental | □ |

3.0E-3

2.0E-3

1.0E-3

0.0

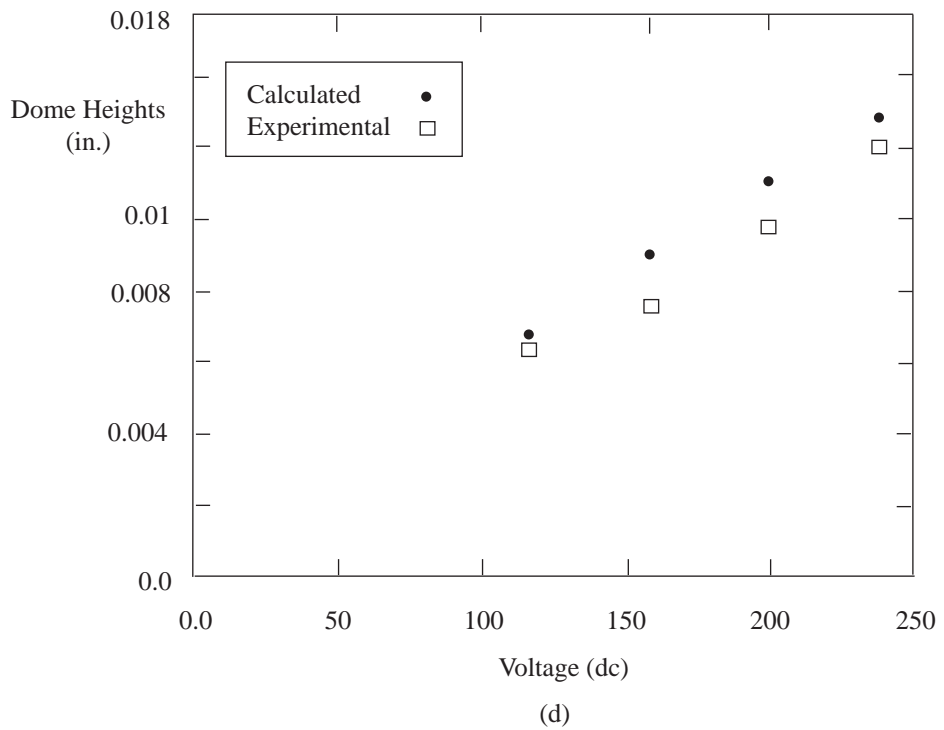0.0   50   100   150   200   250

Voltage (dc)

(b)

Fig. 4 Plots of Comparisons between the Calculated and Experimental results

(c)

(d)

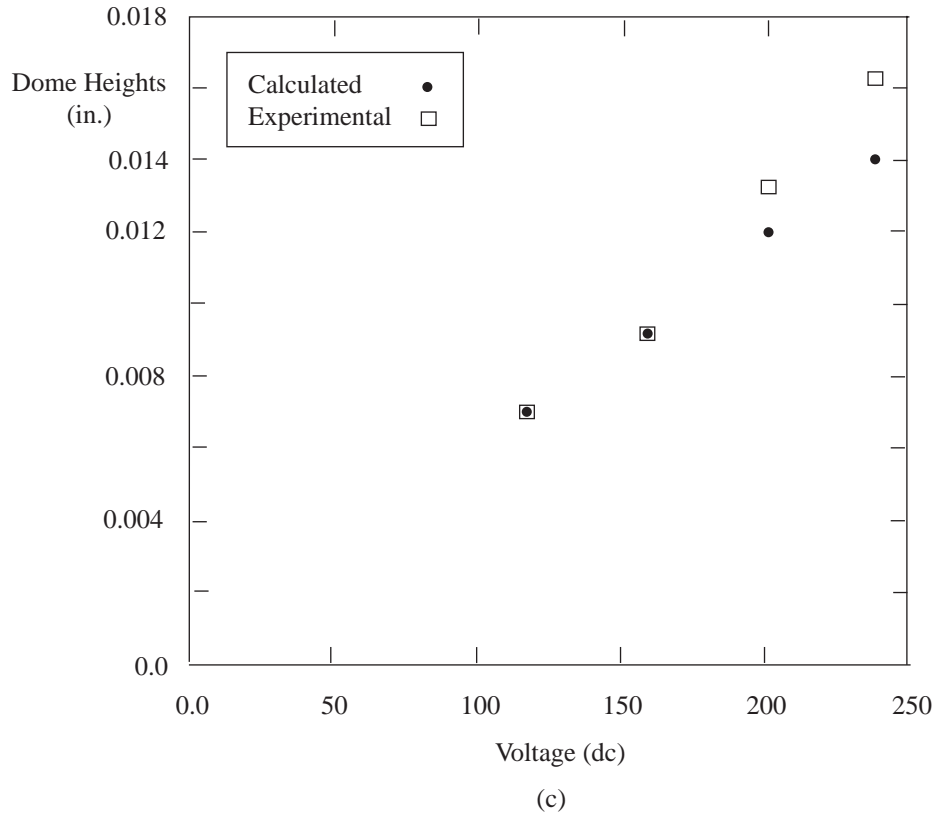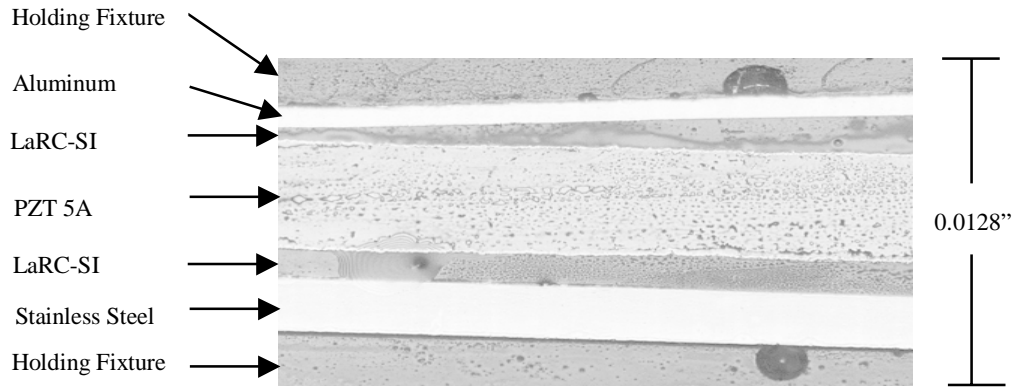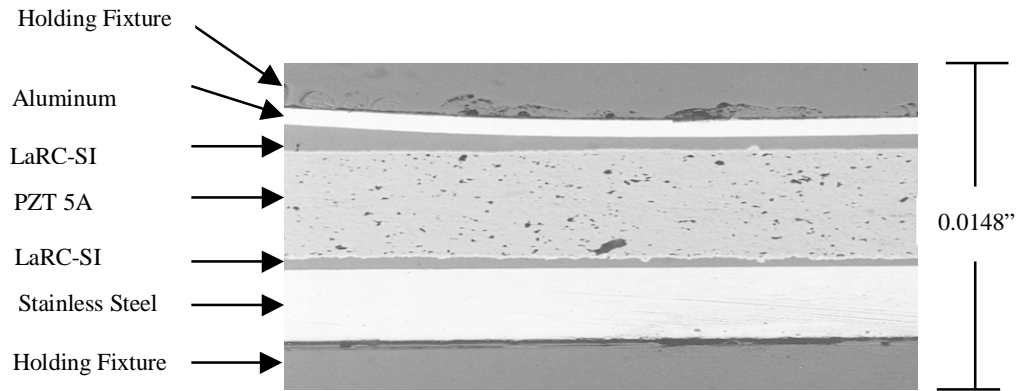Fig. 4 Plots of Comparisons between the Calculated and Experimental results

Holding Fixture
Aluminum
LaRC-SI
PZT 5A
LaRC-SI
Stainless Steel
Holding Fixture

0.0128"

(a) Sample I

Holding Fixture
Aluminum
LaRC-SI
PZT 5A
LaRC-SI
Stainless Steel
Holding Fixture

0.0148"

(b) Sample II

Fig. 5 Cross-Sections of THUNDER Specimens